White light emission in Pr^{3+}, Tb^{3+}:$CaYAlO_4$ phosphor*

CHEN Qiao-ling (陈巧玲) **and LÜ Shao-zhen** (吕少珍)**

Fujian University of Technology, Fujian 350007, China

In this work, the synthesis and photoluminescence characteristics of two new phosphors Pr^{3+}: $CaYAlO_4$ (CYA) and Pr^{3+}/Tb^{3+}: CYA for light emitting diodes (LEDs) are investigated. 0.5% (atom percentage) Pr^{3+}: CYA exhibits the largest bright yellow emission by varying the Pr^{3+} concentration, owing to the cross-relaxation process of $^3P_0 + ^3H_4 \rightarrow {}^1G_4 + {}^1G_4$. The energy level diagram in Pr^{3+}: CYA, especially the positions of 4f5d level and $^1S_0$ level, is discussed. By co-doping Tb^{3+} ions, the color coordinates of Pr^{3+}/Tb^{3+}: CYA phosphor can be tuned from yellow to white region. Finally, the strongest luminescence emission with color coordinates of (0.339, 0.364) located in the white region can be obtained in 0.3%Tb^{3+}/0.5%Pr^{3+}: CYA phosphor.

Nowadays, white light-emitting diode (LED) is considered to be the best candidate for the future light source for its cheap, durable, pollution-free and energy-saving characteristics. Praseodymium (Pr) presents an intricate energy-level diagram, thus it becomes a very attractive ion. Praseodymium can generate a variety of emissions from blue to deep infrared wavelengths, such as blue ($^3P_0 \rightarrow {}^3H_4$), green ($^3P_0 \rightarrow {}^3H_5$) and red ($^3P_0 \rightarrow {}^3H_6$) emissions. Usually, Pr^{3+} doped phosphors show intense red emission, as reported by Kavita Mishra[1], Han-Yu Lin[2] and Qiuxia Li et al[3]. Influenced by crystal field, sometimes Pr^{3+} doped phosphors can exhibit white emission by adjusting doping concentration, such as the reported 0.3% Pr^{3+}:BaY_2F_8 phosphor[4], 2% Pr^{3+}: $LaTiNbO_6$[5] and 3% Pr^{3+}:$YAlO_3$[6]. Tb^{3+} is also one of our candidates which usually emits green light due to the intense $^5D_4 \rightarrow {}^7F_5$ transition[7].

Herein, $CaYAlO_4$ (CYA) was chosen as phosphor host material for its good features like good mechanical strength, chemical stability and high thermal conductivity. CYA is iso-structural with K_2NiF_4, with a space group I4/mmm with lattice parameters of a=3.645 1 nm and c=1.187 43 nm[8]. It has been approved to be a promising laser crystal. The properties of rare earth ions like Nd^{3+}, Er^{3+}, Tm^{3+},Yb^{3+} doped CYA crystals have been reported[9-14]. Sm^{3+}: CYA and Eu^{3+}/Tb^{3+}: CYA phosphors have also been investigated earlier[15-17]. However, as a potential phosphor host material, CYA has not been reported with Pr^{3+} doped or Pr^{3+}/Tb^{3+} co-doped in it to our best knowledge.

In this work, the spectroscopic characterizations of two new phosphors of Pr^{3+}: CYA and Pr^{3+}/Tb^{3+}: CYA for LEDs are investigated. Excited by 263 nm, Pr^{3+}:CYA phosphor shows bright yellow emission. When Pr^{3+} ions are highly doped, the color coordinates go into the white region. But its emission intensity is very weak. To tune the color, a co-dopant ion Tb^{3+} is introduced in the CYA phosphor. Finally, by varying the concentration of Tb^{3+} ions, the strongest white luminescence emission with color coordinates of (0.339, 0.364) has been obtained in 0.3% Tb^{3+}/0.5% Pr^{3+}: CYA phosphor. The emission mechanisms in the two phosphors are investigated. The energy transfer mechanism in Pr^{3+}/Tb^{3+}: CYA phosphor is also discussed.

A series of Pr^{3+}, Tb^{3+}: CYA phosphors were synthesized by solid-state reaction. The starting chemicals were Al_2O_3, $CaCO_3$(A.R.grade) and Y_2O_3, Pr_6O_{11}, Tb_4O_7(4N purity). After being weighed according to the stoichiometric composition, all the chemicals were sufficiently ground in agate mortar and sintered at 1 400 ℃ for 24 h. After that, the procedure of grinding and sintering was repeated. Finally, the phosphor powers were obtained. The fluorescence spectra and the relevant lifetime decay curves were recorded at room temperature by Edinburgh Instruments FLS920 and FSP920 spectrophotometer.

The structure of the phosphor powers was analyzed by a power X-ray diffractometer (XRD) (SCXmini) which is operating at 3 kW and using $CuK\alpha1$ (1.540 6 A). It can be noted from Fig.1 that the diffraction peaks are consistent well with CYA (JCPDS 24-0221), which means the obtained phase is CYA without any parasitic phase. The average structural unit distance can be calculated by the Scherrer equation $D=k\lambda/\beta\cos\theta$, where k is the Scherrer constant, λ is the X-ray wavelength, β is the full width at half maximum of the diffraction peak, and the

most intense reflection at $2\theta=33.4°$ is used here. The calculated average structural unit distance is 54.7 nm. Synthesized in the same condition, all samples share the similar XRD pattern. One typical picture is shown in Fig.1.
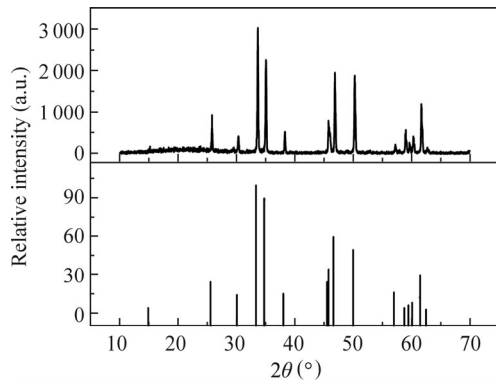
Fig.1 XRD pattern of the as-synthesized CYA phosphors

Fig.2 presents the emission spectra of Pr^{3+}: CYA phosphors excited by 263 nm. Five main fluorescence bands centered around 500 nm, 556 nm, 629 nm, 663 nm and 750 nm can be observed, corresponding to the transitions from the metastable $^3P_0$ to $^3H_4$, $^3H_5$, $^3H_6$, $^3F_2$ and $^3F_{3,4}$ manifolds, respectively. The two most intense emissions are bluish green light at 500 nm and red light at 629 nm.
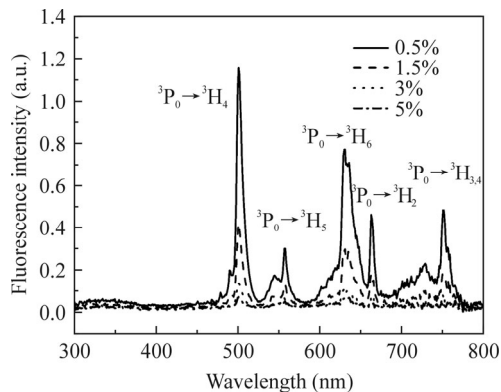

**Fig.2 Fluorescence spectra of 0.5%, 1.5%, 3% and 5% Pr^{3+}: CYA phosphors excited by 263 nm**

Fig.3 displays the excitation spectrum of Pr^{3+}: CYA when monitoring at 629 nm ($^3P_0 \rightarrow {}^3H_4$). A broad excitation peak centered at 260 nm is observed, from which we can deduce that the lowest 4f5d level lies around 3.85×10^3 cm^{-1}. Four weak peaks centered at 451 nm, 478 nm, 489 nm and 498 nm are corresponding to the transitions from $^3H_4$ to $^3P_2$, $^3P_1$, $^3P_0$ and $^1I_6$, respectively.

Generally, the emission of Pr^{3+} ion varies with its host materials for the close energy separation between the low edge of 4f5d configuration and the $^1S_0$ level of 4f^2 configuration. When the lowest 4f5d level lies higher than $^1S_0$ level, such as Pr^{3+}: LaF_3[18], the ions are excited first

to 4f5d level by ultra-violet light and then relax to $^1S_0$ level. Thus, in this case, the emission contains $^1S_0 \rightarrow {}^3P_J$ transitions and then $^3P_0 \rightarrow {}^3H_J$, ^3F_J transitions and $^1D_2 \rightarrow {}^3H_J$ transitions. If the lowest 4f5d level lies lower than $^1S_0$ level, such as Pr^{3+}: YPO_4[18], the emission contains some wide-band peaks which are assigned to 4f5d$\rightarrow$4f^2 transition. In our experiment, the $^1S_0 \rightarrow {}^1I_6$ transition is absent, which is the necessary emission of the two-step intra-configurational transitions. Particularly, it is noted that the 4f5d level energy (3.85×10^3 cm^{-1}) is much lower than those of $CaMgAl_{14}O_{23}$ (50.0×10^3 cm^{-1}) and LaF_3 (53.2×10^3 cm^{-1})[18], in which 4f5d level lies higher than $^1S_0$ level. Thus it can be deduced that the lowest 4f5d level lies lower than $^1S_0$ level in Pr^{3+}: CYA. However, in CYA crystal, the emission bands have no wide-band characteristics. All the emissions belong to the transition within the 4f level. The broad 4f5d$\rightarrow$4f^2 transition wavelength calculated is in 280—400 nm range. So we measured the absorption spectra of Pr^{3+}: CYA phosphors. From the absorption spectra (Fig.4), it is noted that even in the Pr^{3+}: CYA phosphor sample after annealing, intense absorption still exists in the range of 200—400 nm. Thus we believe that the absence of broad 4f5d$\rightarrow$4f^2 transition is due to the absorption of CYA host.
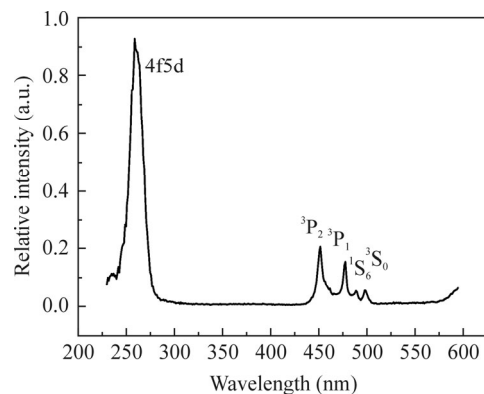

Fig.3 Excitation spectrum of Pr^{3+}: CYA when monitoring at 629 nm
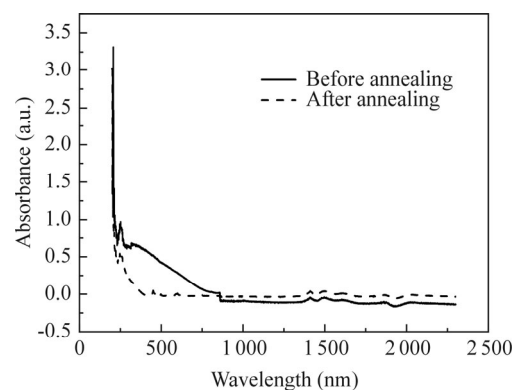
Fig.4 Absorption spectra of Pr^{3+}: CYA phosphors before and after annealing

The emission mechanism can be described as follows: as shown in Fig.5, when Pr^{3+}: CYA is pumped by 263 nm, ions are excited to 4f5d level. Then the ions in 4f5d level relax to the lower levels. Among these emissions, the broad 4f5d→4f^2 emission is absent for the absorption of CYA host, while the ions in 4f5d level can also relax to ^3P_J manifolds and then quickly relax to $^3P_0$ level. After that, the ions in $^3P_0$ level relax to lower ^3H_J and ^3F_J levels to generate emissions like 500 nm and 556 nm.
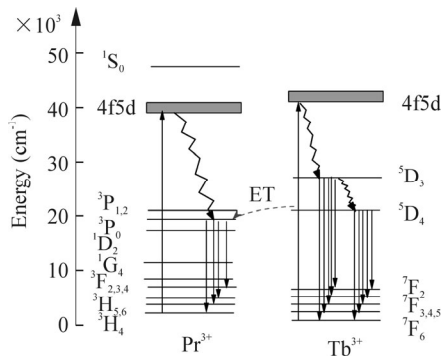

Fig.5 Energy level diagram of Pr^{3+}, Tb^{3+}: CYA and the proposed mechanism

The emission spectra varying with Pr^{3+} doping concentration excited by 263 nm are also presented in Fig.2. It is observed that 0.5% Pr^{3+}: CYA has the largest fluorescence emission. As the doping concentration increases, the fluorescence intensity decreases quickly. The concentration quenching is probably due to the cross-relaxation processes. When Pr^{3+} ions are heavily doped, the distance between ions is getting smaller, and thus the probability of cross-relaxation processes increases. The cross-relaxation process $^3P_0 + ^3H_4 \rightarrow ^1G_4 + ^1G_4$[6] causes the depopulation of $^3P_0$ level and finally leads to the much weaker emission in highly doped sample.

As one of the important factors for evaluating phosphors performance, color coordinates are calculated according to the CIE standard. They are (0.401, 0.416), (0.407, 0.448), (0.411, 0.423) and (0.385, 0.378) for 0.5%, 1.5%, 3% and 5% Pr^{3+}: CYA phosphors, respectively and marked in Fig.6. Basically, the color coordinates are located in yellow region. When Pr^{3+} ions are heavily doped, such as 5%, the color ordinates are switched towards white region. It implies the possibility of Pr^{3+}: CYA phosphor as a promising LED material which emits yellow light and can be effectively pumped by UV 263 nm light.

We note that when Pr^{3+} ions are highly doped (5%), the color coordinates go into the white region. However, its emission intensity is very weak (seen in Fig.2) due to the cross-relaxation process of $^3P_0 + ^3H_4 \rightarrow ^1G_4 + ^1G_4$. To tune the light color, we study a series of co-doped Pr^{3+}/Tb^{3+}: CYA phosphors. Fig.7 gives the emission spectra of co-doped Pr^{3+}/Tb^{3+}: CYA phosphors with four

different Tb^{3+} doping concentrations. By comparing the emission spectra of Pr^{3+}: CYA phosphors, it is noted that the main emission peaks are corresponding to the 4f-4f transitions of Pr^{3+} ions, and no intense emission peaks of Tb^{3+} ions are observed. Of course, some differences between the emission spectra of Pr^{3+}: CYA and Pr^{3+}/Tb^{3+}: CYA phosphors still exist. This indicates that the energy transfers from Tb^{3+} to Pr^{3+} ions.
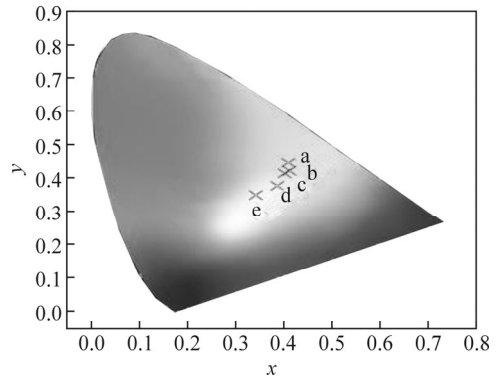
Fig.6 CIE coordinates for Pr^{3+}: CYA phosphor (a: 0.5%; b: 1.5%; c: 3%; d: 5%) excited by 263 nm and Pr^{3+}/Tb^{3+}: CYA phosphor (e: 0.3% Tb^{3+}, 0.5% Pr^{3+}) excited by 254 nm
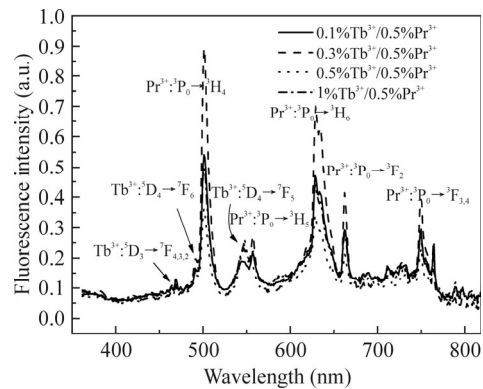

Fig.7 Fluorescence spectra of Pr^{3+}/Tb^{3+}: CYA phosphors excited by 254 nm

To verify this suggestion, Tb^{3+}: CYA phosphor was also synthesized and investigated. Fig.8 gives the emission spectrum of 0.3% Tb^{3+}: CYA phosphor. Fluorescence bands are centered at 382 nm, 415 nm, 438 nm, 468 nm, 489 nm, 547 nm, 589 nm and 623 nm, corresponding to the transitions of $^5D_3 \rightarrow ^7F_6$, $^5D_3 \rightarrow ^7F_5$, $^5D_3 \rightarrow ^7F_4$, $^5D_4 \rightarrow ^7F_6$, $^5D_4 \rightarrow ^7F_5$, $^5D_4 \rightarrow ^7F_4$ and $^5D_4 \rightarrow ^7F_3$, respectively. The absorption spectrum of Pr^{3+}: CYA phosphor is also presented in Fig.8 for comparison.

According to energy transfer theory, if there is the overlapping between the absorption band of activator and the emission band of the sensitizer, the energy transfer between them is likely to occur, and because of that, the luminescence lifetime of sensitizer will be shorten. From Fig.8, it is found that two large overlapped bands are

around 489 nm and 600 nm, which are corresponding to the emission from the $^5D_4$ state of Tb^{3+} ion and the absorption of $^1I_6$, $^3P_0$ state of Pr^{3+} ion[19]. Although the absorption intensities of peaks located at 452 nm and 478 nm are large, the emissions at these wavelengths are much weaker. So the energy transfer between Tb^{3+}:$^5D_3$ and Pr^{3+}:^3P_J may exist, but probably the energy transfers mainly between Tb^{3+}:$^5D_4$ and Pr^{3+}:^3P_J levels, which involves these two processes: Tb^{3+}: $^5D_4 + Pr^{3+}$: $^3H_4 \rightarrow Tb^{3+}$: $^7F_6 + Pr^{3+}$: $^1I_6$ and Tb^{3+}: $^5D_4 + Pr^{3+}$: $^3H_4 \rightarrow Tb^{3+}$: $^7F_4 + Pr^{3+}$: $^3P_0$.
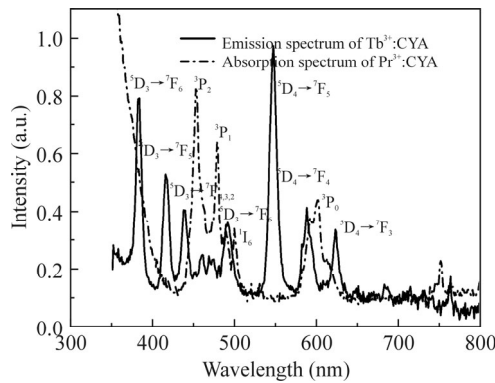
Fig.8 Emission spectrum of Tb^{3+}: CYA phosphor and absorption spectrum of Pr^{3+}: CYA phosphor in the range of 350—800 nm

To analyze the energy transfer between Tb^{3+} and Pr^{3+} ions in Pr^{3+}/Tb^{3+}: CYA phosphor, the decay curves of Tb^{3+}:$^5D_4$ level in Tb^{3+}: CYA and Pr^{3+}/Tb^{3+}: CYA phosphors excited by 254 nm were measured. Fig.9 presents the lifetime decay curves of 489 nm emission in 0.1% Tb^{3+}: CYA and 0.5% Pr^{3+}/0.1% Tb^{3+}: CYA phosphors. In lowly doped Tb^{3+}: CYA samples (0.1% Tb^{3+}: CYA, 0.3% Tb^{3+}: CYA), the lifetime curves are singly exponential, while in highly doped sample and co-doped sample, owing to concentration quenching effect and energy transfer process, the lifetime decay curves show non-exponential characteristic. Lifetime τ can be calculated by an integrating method:

$$\tau = \int_0^\infty \frac{I(t)}{I_0} \, \mathrm{d}t , \tag{1}$$

where $I(t)$ is the emission intensity at 489 nm as a function of time t, and I_0 is the initial intensity. Besides, the energy transfer efficiency is calculated using the following formula:

$$\eta = 1 - \tau_{DA} / \tau_D , \tag{2}$$

where τ_{DA} is the lifetime of the donor in the presence of the acceptor, and τ_D is the lifetime of the donor in the absence of the acceptor. The measured lifetimes in different Tb^{3+} doped CYA phosphors and Tb^{3+}/Pr^{3+} co-doped samples are listed in Tab.1, as well as the calculated energy transfer efficiency.
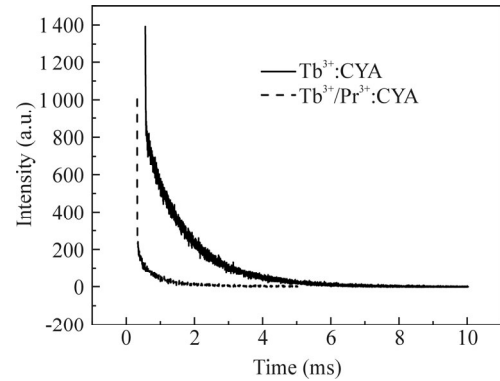
Fig.9 Decay curves of 0.1% Tb^{3+}: CYA and Pr^{3+}/Tb^{3+}: CYA phosphors recorded at 489 nm

Tab.1 Lifetime and the energy transfer efficiency in different Tb^{3+} doped and Tb^{3+}/Pr^{3+} co-doped samples

Phosphor	Lifetime (ms)	Energy transfer efficiency η
0.1% Tb^{3+}: CYA	1.126	0.81
0.1% Tb^{3+}/0.5% Pr^{3+}: CYA	0.23	
0.3% Tb^{3+}: CYA	1.185	0.90
0.3% Tb^{3+}/0.5% Pr^{3+}: CYA	0.107	
0.5% Tb^{3+}: CYA	0.987	0.79
0.5% Tb^{3+}/0.5% Pr^{3+}: CYA	0.20	
1% Tb^{3+}: CYA	0.895	0.87
1% Tb^{3+}/0.5% Pr^{3+}: CYA	0.122	

It can be noted from Tab.1 that the lifetime of 489 nm emission in co-doped sample, which is associated with the $^5D_4 \rightarrow \ ^7F_6$ of Tb^{3+} ion, decreases drastically compared with that in singly Tb^{3+} doped sample. That means the energy effectively transfers from Tb^{3+} ion to Pr^{3+} ion. Besides, the energy transfer efficiency is high. So in the emission spectrum of Pr^{3+} / Tb^{3+}: CYA phosphor, the intense luminescence peaks belong to the transition of Pr^{3+} ion, and only some weak peaks, such as 468 nm, 489 nm and 547 nm, are corresponding to the emission of Tb^{3+} ion. In the four co-doped Pr^{3+}/Tb^{3+}: CYA phosphors, the 0.3% Tb^{3+}/0.5% Pr^{3+}: CYA has the largest energy transfer efficiency, while the 0.5% Tb^{3+}/0.5% Pr^{3+}: CYA has the least value. These coincide well with the emission intensities of Pr^{3+} / Tb^{3+}: CYA phosphors shown in Fig.7. Among the four Pr^{3+} / Tb^{3+}: CYA phosphors with different doping concentrations, the 0.3% Tb^{3+}/0.5% Pr^{3+}: CYA has the largest energy transfer efficiency (0.90). In other words, most energy transfers from Tb^{3+}:$^5D_3$ to Pr^{3+}:^3P_J level, which finally results in the largest emission peak intensity originating from Pr^{3+} ion.

Color coordinates of the 0.3% Tb^{3+}/0.5% Pr^{3+}: CYA phosphor emission are calculated to be (0.339, 0.364). It is located in the white region as shown in Fig.6. So, by co-doping Tb^{3+} ions, owing to the increasing emission in the short wavelength, the color coordinates of Pr^{3+}: CYA phosphor can be tuned from yellow to white region.

In conclusion, a series of Pr^{3+}: CYA and $Pr^{3+}/$ Tb^{3+}: CYA phosphors were synthesized and investigated. Excited by 263 nm, the Pr^{3+}: CYA phosphor exhibits bright yellow luminescence. The experimental results show that the 4f5d level lies lower than $^{1}S_0$ level in Pr^{3+}: CYA and the absence of 4f5d→$4f^2$ transition is ascribed to the absorption of CYA host. White color emission can be obtained by co-doping Tb^{3+} ions in Pr^{3+}: CYA phosphor. The energy transfer mechanisms of Pr^{3+}/Tb^{3+}: CYA phosphor are investigated. By varying the concentration of Tb^{3+} ions, the strongest white luminescence emission with color coordinates of (0.339, 0.364) can be obtained in the 0.3% Tb^{3+}/0.5% Pr^{3+}: CYA phosphor.

References

[1] Kavita Mishra, Y. Dwivedi, A. Rai and S. B. Rai, Phys. B **109**, 663 (2012).

[2] Han-Yu Lin, Fu-Chang Wei and Yuan-Chu Sheng, Journal of Luminescence **133**, 194 (2013).

[3] Su Zhang, Hongbin Liang and Chunmeng Liu, J. Phys. Chem. C **117**, 2216 (2013).

[4] A.Toncelli, L. Bonelli, R. Faoro, D. Parisi and M. Tonelli, Optical Materials **31**, 1205 (2009).

[5] Xiao-ding Qi, Chieh-Min Liu and Chung-Chiang Kuo, Journal of Alloys and Compounds **492**, 61 (2010).

[6] Yuexia Ji, Jiafeng Cao and Zhaojie zhu, Materials Express **1**, 231 (2011).

[7] Z. Kotan, M. Ayvacikli, Y. Karabulut, J. Garcia-Guinea, L. Tormo, A. Canimoglu, T. Karali and N. Can, Journal of Alloys and Compounds **581**, 101 (2013).

[8] D.Z. Li, X.D. Xu, S.S. Cheng, D.H. Zhou, F. Wu, Z.W. Zhao, C.T. Xia, J. Xu, J. Zhang, H.M. Zhu and X.Y. Chen, Appl. Phys. B **101**, 199 (2010).

[9] Dongzhen Li, Xiaodong Xu, Yan Cheng, Shishu Cheng, Dahua Zhou, Feng Wua, Changtai Xia, Jun Xu and Jian Zhang, Journal of Crystal Growth **312**, 2117 (2010).

[10] P.O. Petit, J. Petit, Ph. Goldner and B. Viana, Optical Materials **30**, 1093 (2008).

[11] R. Moncorge, N. Garnier, Ph. Kerbrat, Ch. Wyon and C. Borel, Optical Communications **141**, 29 (1997).

[12] Horacio R, Verdun and Leonard M, Thomas, Appl. Phys. Lett. **56**, 7 (1990).

[13] J.C. Souriau, C. Borel, Ch. Wyon, C. Li and R. Moncorge, Journal of Luminescence **59**, 349 (1994).

[14] J. Andrew Hutchinson, Horacio R. Verdun, Bruce H.T. Chai, Bahram Zandi and Larry D. Merkle, Optical Materials **3**, 287 (1994).

[15] Myung Sub Kim and Jae Su Yu, Phys. Status Solidi B **250**, 374 (2013).

[16] Geng Dongling, Li Guogang and Shang Mengmeng, Dalton Transactions **41**, 3078 (2012).

[17] Kim Myung Sub, Bharat L. Krishna and Yu Jae Su, Journal of Luminescence **142**, 92 (2013).

[18] Fangtian You, Shihua Huang, Chunxia Meng, Dawei Wang, Jianhua Xu, Yan Huang and Guobin Zhang, Journal of Luminescence **122-123**, 58 (2007).

[19] G. Ozen, O. Forte and B. Di Bartolo, Journal of Applied Physics **97**, 013510 (2005).